

Electrochemical Synthesis in Microreactors

Kevin Watts, Alastair Baker and Thomas Wirth*

School of Chemistry, Cardiff University, Park Place, Main Building, Cardiff CF10 3AT, UK

Different electrochemical microreactors for continuous flow synthesis are described in this review. Advantages of flow over batch type chemistry are highlighted as well as novel developments in construction of such devices.

1. Introduction

Over the last 10 to 20 years, a huge increase in interest of electroorganic chemistry has been observed. This is not only due to the advances in equipment and understanding of electrochemical reactions, but also because of the advantages it can offer to organic synthesis [1–4].

Electrochemistry is an efficient and clean method for the use of electrons in organic chemistry and reactive species, such as radicals, radical-ions, carbanions as well as carbocations can serve as intermediates in reactions. The electricity supplied to the electrodes causes the formation of these reactive intermediates from neutral substrates. As electrons are the ‘reagent’, these processes become cheaper, often more selective and less labour intensive.

Conventional batch chemistry is often held back by thermodynamics. More energy is required to heat large batch syntheses than is required for electrochemistry. Through electrochemistry, a precise control of the electrical current applied between the electrodes can be achieved, allowing reactions to be carried out under milder reaction conditions compared to conventional organic chemistry. As electricity is relatively cheap and widely available in comparison to most other reagents, electrosyntheses are very promising chemical processes. Furthermore, electrochemistry can suit continuous processes considering a reaction can be run as long as electricity is supplied to the reaction vessel.

There are also some disadvantages to electrochemical processes as only certain combinations of solvent and supporting electrolyte can be used to enable reactions by carrying charges through the cell. These can be expensive and typically require an aqueous work-up after electrosynthesis is finished. Cooling is often necessary as overheating can occur due to the design of a batch cell which causes inhomogeneities of temperature throughout the cell. This can lead to the formation of “hot-spots” and “dead zones” due to poor mass and heat transfers often associated with a batch cell (Figure 1).

The development of electrochemical microreactors (ECMR's) was a logical extension as the field of microreactors and continuous flow chemistry evolution has occurred in the last two decades. The platform that microreactors offer is perfect for this aim, miniaturising traditional flask chemistry, reducing amounts of solvents and substrates and making process optimisation much less wasteful developments. A factor that has led to the vast and rapid expansion of flow chemistry is the availability of commercial microreactor equipment, both chip reactors and other modular devices. Its expansion through chemistry is evident within areas such as medicinal chemistry, with PET (positron emission tomography) tracers being synthesised in microreactors [5], and in the fine chemical and pharmaceutical industries [6].

2. Advantages of Electrochemical Microreactors (ECMR's)

Disadvantages of conventional batch electrochemistry include factors such as a non-homogeneous electrical field in the reaction

vessel causing “hot-spots” in the reaction solution, and the necessity to add supporting electrolytes to the reaction solution to improve current flow through the reaction mixture.

Microreactors for electrosynthesis have been designed to overcome these limitations inherent of conventional electrochemistry. The presence of “hot spots” during the reaction has been eliminated as the reaction solution flows between the electrodes so a homogeneous current density is obtained. Figure 1 illustrates these effects and compares them with conventional batch reactions [7,8].

The high surface-to-volume ratio of electrode area to the reaction volume and the close proximity of the electrodes also allow for more efficient reactions. The close proximity of the electrodes negates the presence of a large current gradient as present in a batch reactor (Figure 1a). This produces the ability to conduct electrochemistry without the use of supporting electrolytes because the two diffusion layers of the electrodes are able to overlap. The ions generated at the electrode surfaces are able to diffuse through the solution and carry the electrical charge to complete the electrical circuit [9,10].

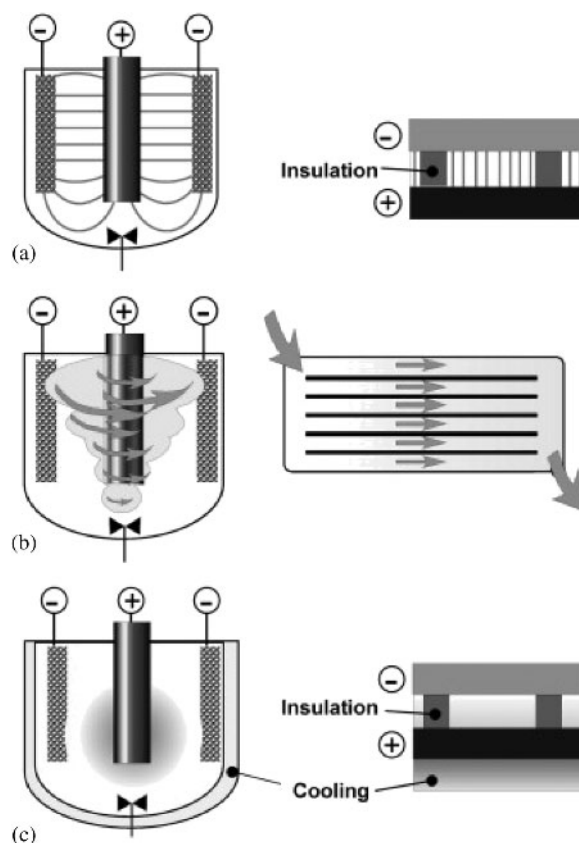


Figure 1. Batch/flow comparison. (a) Current distribution, (b) Mass transfer and (c) Heat transfer (Reprinted from ref. [8] with permission from Elsevier)

* Author for correspondence: wirth@cf.ac.uk

Different types of microreactor electrodes “set-ups that have been designed, primarily undivided and divided cells, are used for preparative electrochemical synthesis in microreactors. It is important to mention that other electrochemical devices have been designed and developed for electrochemical sensing and there are reviews available such as those by Stradiotto et al. [11] and Janata et al. [12]

3. Undivided Cells

3.1. Solid Electrode Plate to Plate Geometries. The most basic type of cell construction is that of an undivided cell for constant current electrolysis. A simple batch cell of this type comprises of an unsealed glass beaker and two electrodes which are generally used for reactions where the products will not react with the other electrode. Such a reaction, for example, is the Kolbe electrolysis. The electrodes are placed as close to each other as possible to reduce the resistance of the cell and more electrodes can be set in parallel to produce a larger working electrode surface. The most common type of electrodes are solid metal, separated by a non-conducting spacer to form a reaction channel. The electrodes are positioned in a plate to plate geometry as shown below (Figure 2). [1,13,14]

Nonaka et al. [15] reported one of the earliest electrochemical synthesis in an ECMR. The authors investigated product-selectivity of the reaction by controlling the mass-transfer rate of the reactions. The microreactor used was supplied by Electrocell AB, Sweden and consisted of a lead plate cathode and a ruthenium oxide-coated titanium anode (3.3 x 3.3 cm) and separated by a Nafion® cation-exchange membrane. They showed that flow rate, current density and substrate concentration had an effect on the product formation. In addition they included a comparison of the rotation speed of a lead cathode to the batch process. The results indicated that by controlling the mass transfer rates, the selectivity of the reactions between the hydrodimer and hydro-monomer can be controlled, and in the best case of benzophenone a ratio of 70:1 in favour of the desired hydrodimer was achieved.

Subsequently the anodic trifluoromethylation of olefins in flow was published (Scheme 1) [16]. Both electrodes of the ECMR were modified to being made from platinum. Again the effects of mass transfer rates of the reaction were investigated with regard to the current efficiencies. Three substrates **1** were investigated with varying results; With acrylamide **1a** as the substrate, a maximum yield and current efficiency of 48 and 17%, respectively of the monomeric product **2**, with their results

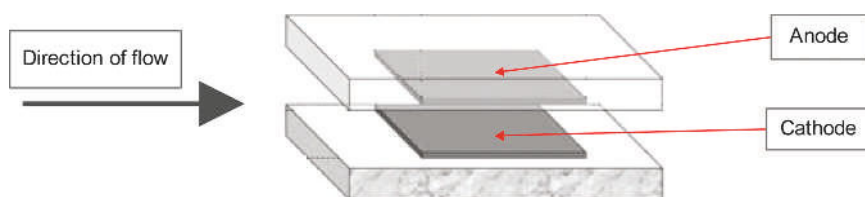
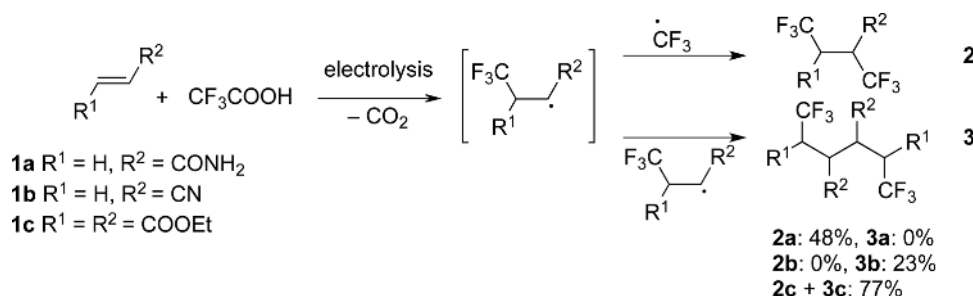
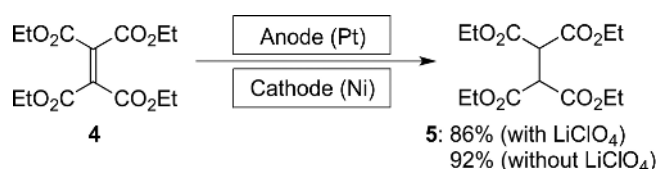


Figure 2. Schematic representation of a plate to plate electrochemical microreactor (With kind permission from Springer Science+Business Media: ref. [9])

Scheme 1. Trifluoromethylation of olefins in an ECMR



Scheme 2. The two electron/two proton reduction of **4**



indicating that the reaction was not affected by mass transfer. By changing the substrate to acrylonitrile **1b**, the exclusive product was found to be the dimer **3**, and with diethyl fumarate **1c**, both products were observed. The results indicated that greater current efficiencies could be increased with an increase in concentration of the substrates. It is also worth noting the yields achieved were greater than that recorded in a batch cell.

Löwe and Ehrfeld reported the methoxylation of 4-methoxytoluene in the presence of KF as a supporting electrolyte [17]. The authors were able to improve the selectivity of the reaction with regards to 4-methoxybenzaldehyde from approximately 85% in common industrial processes to >98% in their ECMR.

Paddon et al. [18] have created an ECMR for the two electron/two proton reduction of **4** dissolved in ethanol (Scheme 2). Comparison with and without supporting electrolyte showed that higher yields of **5** were obtained without supporting electrolyte (86% and 92%, respectively). The choice of cathode was nickel because initial reaction tests proved that the reaction proceeded more efficiently than when platinum cathodes were used.

Scheme 3. The anodic methoxylation of furan **6**



A similar setup for the anodic methoxylation of furan **6** was designed by Atobe et al. [19] (Scheme 3). They compared different electrode configurations to maximise the yield for the reaction, their best result was achieved when a glassy carbon (GC) anode was paired with a platinum cathode. Optimisation of the reaction conditions led to an almost quantitative conversion of **6** with a current density of 3 mA cm^{-2} and a range of flow rates between $0.01\text{--}0.1 \text{ ml min}^{-1}$. The cell was simply constructed with

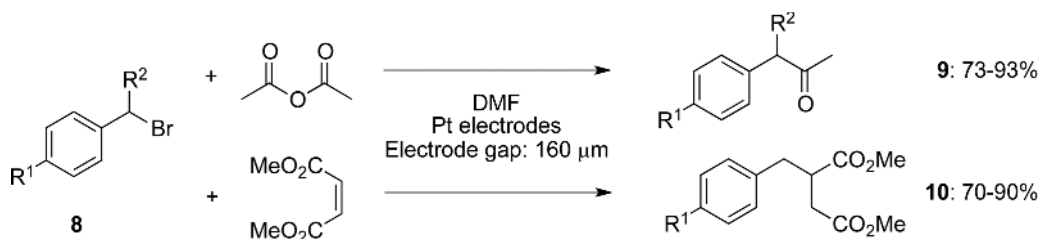
Scheme 4. Electroorganic syntheses carried out in an ECMR by Haswell et al. [20–23]

plate electrodes (3 cm x 3 cm) separated by an adhesive tape (80 μm thick) to create a centre channel with an area of 1 x 3 cm^2 , sandwiched together and sealed with an epoxy resin. The workup after the reaction is a one-step procedure; the solvent is removed together with excess **6** to give pure product **7**.

Haswell et al. [20] report the cathodic coupling of 4-nitrobenzylbromide (Scheme 4). The microreactor consisted of two platinum foil electrodes (25 mm squares, 50 μm thickness) separated by a polytetrafluoroethylene (PTFE) spacer creating a reaction channel, and sandwiched together between two glass plates (forming the top and bottom of the device) which contained holes to create inlet and outlet for the reaction solution and it was all clamped together. The device was then sealed with a silicon adhesive to prevent leaking. The authors investigate the flow rate, current density and inter-electrode distances (160/320 μm) for the reaction. In this case the larger electrode distance generates the highest yields. This is explained due to the closer electrode distance allowing the anode to cause some interference in the reaction. This leads to a larger amount of the monomeric side product (4-nitrotoluene) to be formed via formation of a neutral 4-benzyl bromide radical reacting with a proton generated at the anode. The

best results achieved were 92% conversion with a 91:9 ratio of dimeric product to monomeric side product.

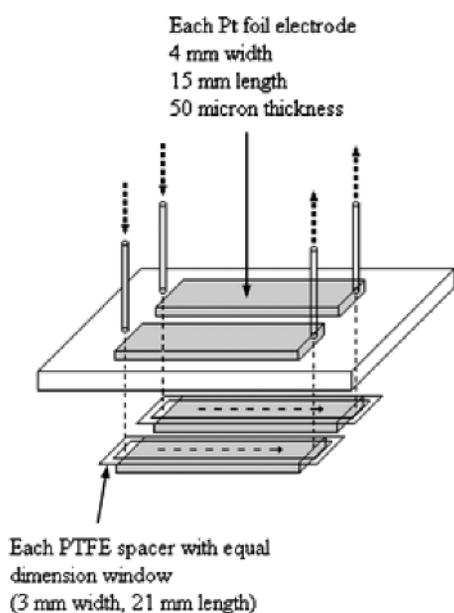
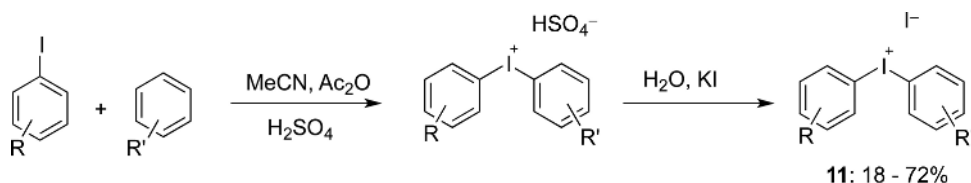
The same group also report the self-supported coupling of activated olefins with benzyl bromides **8** (Scheme 4) using the same microreactor configuration and varying the same parameters [21]. Better results were achieved when the electrodes were closer, allowing a lower voltage and resulting in conversions of >90%. At a larger electrode distance (320 μm), conversions of 47% and 77% were achieved, with an increase in current only growing the amount of homo coupling products. Yields of up to 99% were achieved with a selection substituted benzyl bromides and activated olefins.

Subsequently, the scaling up of the synthesis was reported [22]. The ECMR was modified to be able to support two different microreactor electrode set-ups which increased the number of reaction channels per electrode (Figure 3). Four configurations were tested, 1 electrode with 2 channels, 2 electrodes with 2 channels, 4 electrodes with 4 channels and 1 electrode with 4 channels. With the exception of the latter, all configurations using **8** as a substrate gave 97–98% yield in each of the parallel reactors highlighting the ease at which reactions in ECMR's can be achieved.

Haswell et al. [23] also used the same single cell microreactor configuration to show the ability to synthesise pharmaceutically important intermediates in flow. Specifically, the reactions of benzylbromide derivatives **8** were investigated as shown in Scheme 4. Using an inter-electrode gap of 160 μm gave better yields than a larger distance for the coupling of benzyl bromide derivatives with activated olefins. Coupling reactions with acetic anhydride to arylacetone compounds **9** and with maleic ester to derivatives **10** were reported.

Wirth et al. [24] have reported the formation of both symmetrical and unsymmetrical diaryl iodonium salts **11** in an ECMR on platinum electrodes (Scheme 5). The coupling reaction between an arene and an iodoarene were investigated. Sulfuric acid present in the reaction acted both as a counter ion to the intermediate formation of diaryl iodonium hydrogen sulfates, it also acts as an electrolyte to carry charge through the solution.

Purification of the iodide salt products **11** was not necessary as the diaryl iodonium iodide salts precipitated out of solution once potassium iodide was added. One advantage of the ECMR described is that it is easily dismantled and reassembled unlike many of the other examples which are sealed completely. If electrode soiling or blockage occurs, the problem can be easily rectified (Figure 4).

**Figure 3.** A schematic representation of a 2 electrodes with 2 channels parallel microreactor set up (Reproduced from ref. [22] with permission of The Royal Society of Chemistry)**Scheme 5.** Formation of diaryl iodonium salts in an ECMR

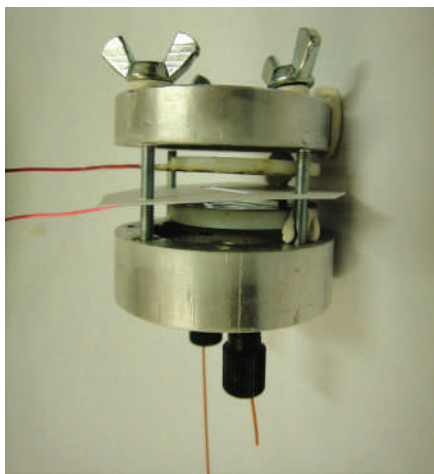


Figure 4. An exploded photograph of an ECMR by Wirth et al. (Taken from ref. [24])

Birkin et al. [25] reported the fabrication of a simple and inexpensive microreactor developed for the methoxylation of *N*-formylpyrrolidine **12** and 4-*tert*-butyltoluene **13** (Scheme 6). The reactor is constructed in a circular design (100 mm diameter) with a graphite plate anode and a stainless steel cathode. The spacer forming the reaction channel was laser cut in a star shape out of Viton, a fluoropolymer elastomer, giving a total channel length of 600 mm (Figure 5). The methoxylation of *N*-formylpyrrolidine was optimised to give conversions of up to 96% with an isolated yield of 87% of product **14**. The oxidation of 4-*tert*-butyltoluene **13** was less successful in terms of yields and conversions with a 64% conversion leading to product yields of 39% and 25% of the ether **15** and acetal **16**, respectively, with a cell current of 50 mA. The cell current was reported to be below that required for full mass transport control, which is also the reason for the high yield of the aldehyde side product. Conversions were increased by either reducing the flow rate or increasing the applied current but no improvement in selectivity was observed.

The same authors used the anodic methoxylation of *N*-formylpyrrolidine again to design and fabricate a microreactor which is more suitable for a saleable commercial flow package that would appeal to the non-electrochemist [26]. The aim was to create a device further miniaturised than the previous one (Figure 5), easier and more convenient to use so as to be more accepted by traditional organic chemists. They also wanted a high single pass conversion of the substrate, to achieve this they changed their circular design to a rectangular shape and incorporated a “snaking” channel design into the spacer, creating a channel length of 700 mm (Figure 6) and a working electrode area of 1050 mm². With this new design, they were able to increase the previous

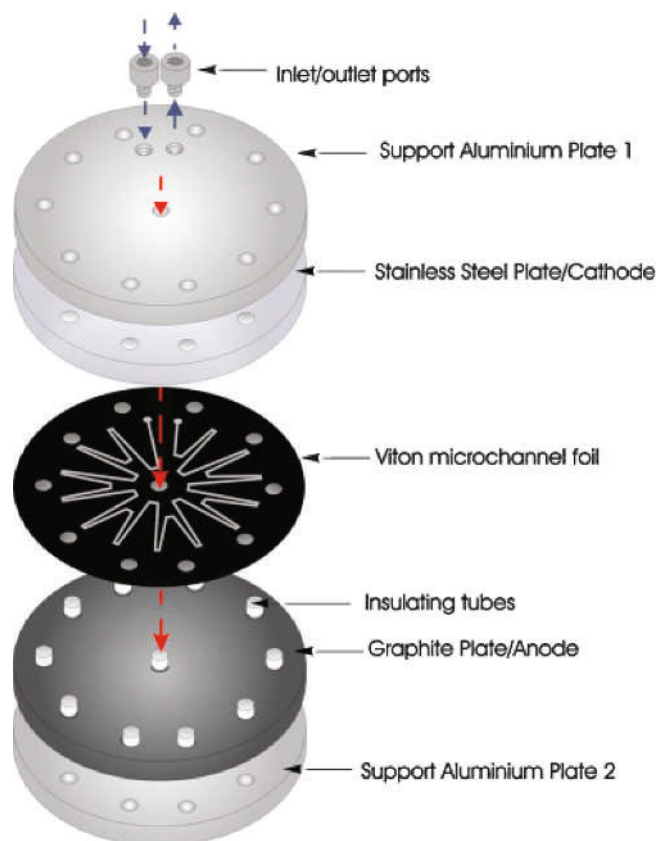


Figure 5. A simple electrochemical microreactor designed to give an elongated channel length (Reprinted from ref. [25] with permission from Elsevier)

conversion to >90% in most cases, and with a high purity of product without any organic side products.

A microreactor designed and fabricated by Roth et al. [27] has been used to investigate four- and six-electron benzylic oxidations. The reactor electrodes range from carbon fluoropolymer (PVDF) hybrids, to stainless steel and platinum, separated by a gasket similar to that in Figure 6, with the device capable of handling pressures of up to 6.5 bar and temperatures from 0 to 65 °C. The authors carry out experiments on toluene derivatives and vary flow rates, electrode materials and the number of electrons (F mol⁻¹) transferred to the substrate. A supporting electrolyte is used for many of the syntheses, but the oxidation of *p*-methoxy toluene is investigated in the absence of any supporting electrolyte. The selectivities and yields of the reactions are poor to reasonable in most cases, with the highest yield of *p*-methoxy dimethylacetal 64% achieved in the electrolyte-free synthesis, with 33% and 3%, respectively of the corresponding aldehyde and ester. They conclude that not one general protocol can be effective for a variety of electron rich and deficient aromatics and each substrate requires individual optimisation to achieve the highest yields.

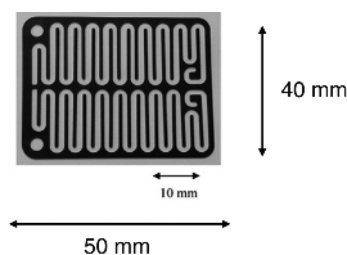
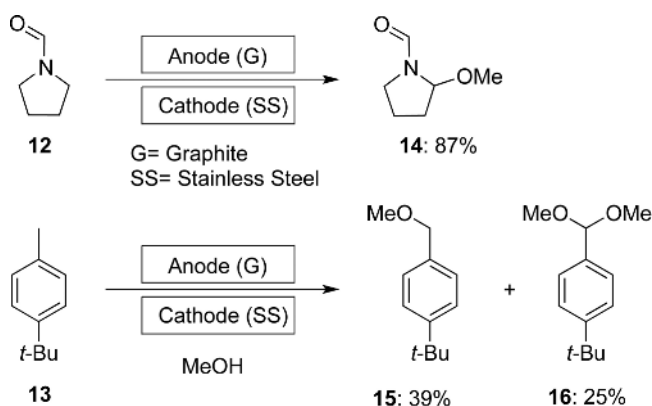
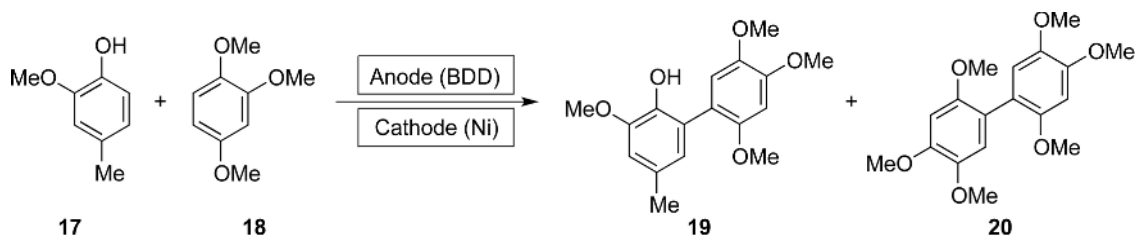
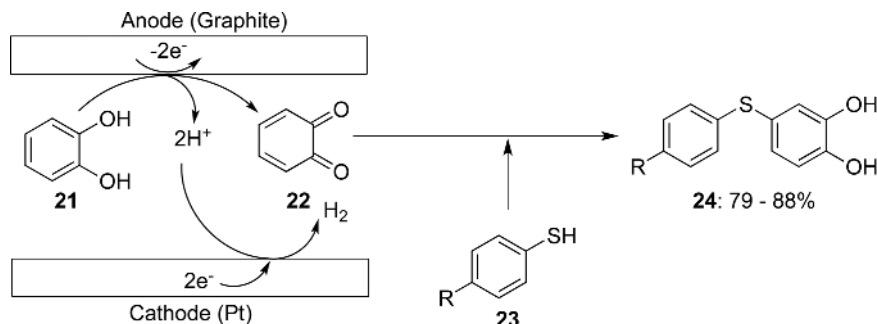
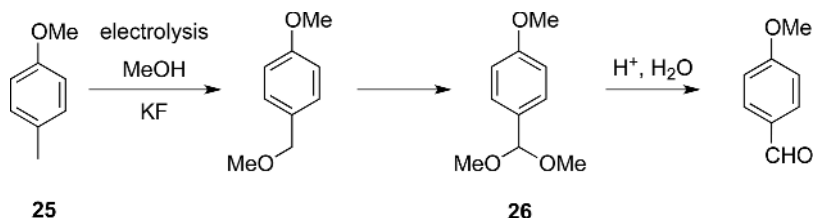


Figure 6. A snaking channel design (Reprinted from ref. [26] with permission from Elsevier)

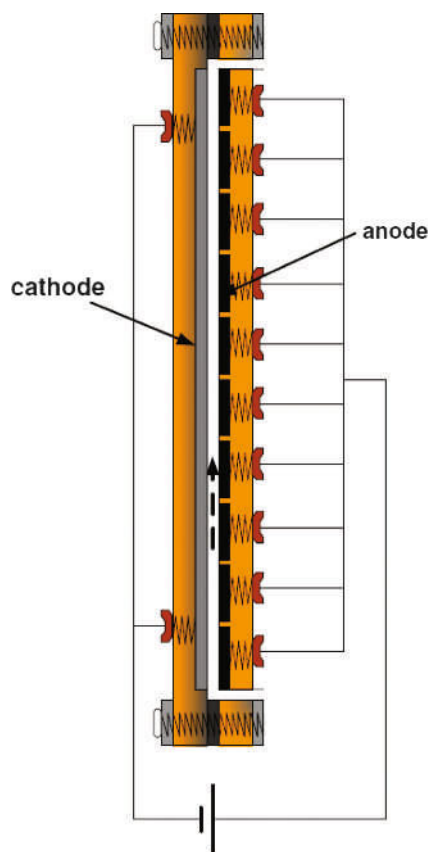
Scheme 6. Anodic methoxylation



Scheme 7. A carbon-carbon cross coupling reaction in flow**Scheme 8.** The use of unstable electrogenerated intermediates and subsequent chemical reactions**Scheme 9.** The selective oxidation of **9** in an ECMR

Carbon-carbon cross coupling reactions have recently been achieved in an electrochemical microreactor consisting of boron-doped diamond (BDD) anode and a nickel cathode reported by Waldvogel et al. [28] The electrodes were separated by both sides using adhesive tape as previously described, to leave a reactor channel with the dimensions $1 \times 3.5 \text{ cm}^2$. The coupling reaction between **17** and **18** (Scheme 7), gave a total yield of the two coupling products **19** and **20** of 90% at current densities of 2.8 mA cm^{-2} . When acetic acid was used as the solvent owing to the Lewis acidity stabilising the cation radicals, not acting as a nucleophile, and extending the lifetime of the radical, a higher yield was achieved, whereas methanol gave a much lower yield (5%). However, the selectivity of the cross coupling in methanol was >99:1 (**19**:**20**), in contrast to a 1:1.4 ratio in acetic acid.

3.2. Electrogeneration of Unstable Intermediates and Their Sequential Reaction. The ability to generate and subsequently use unstable intermediates is another advantage of electrochemical microreactor synthesis and was reported by Atobe et al. [29] The synthesis of diarylsulfide derivatives was achieved from the generation of the unstable *o*-benzoquinone intermediate **22** (Scheme 8). Compound **22** is generated by the electrochemical oxidation of catechol **21** in the microreactor at the graphite anode, with hydrogen being formed at the cathode. Once the reaction solution leaves the microreactor, it joins a stream of a thiophenol derivative **23** and undergoes a rapid Michael addition giving the product. The best results obtained were with an isopropyl substituted thiophenol **23** ($R=i\text{-Pr}$) and the electrogenerated intermediate **22** leading to **24** in a yield of 88%, this compared to a batch type reaction with 13% yield. The electrode distance was $80 \mu\text{m}$ with a current density of 1.5 mA cm^{-2} . This, however, is not an unsupported synthesis, as the authors report the use of sodium perchlorate as a supporting electrolyte.

**Figure 7.** An undivided cell with a segmented anode (With kind permission from Springer Science+Business Media: ref. [31])

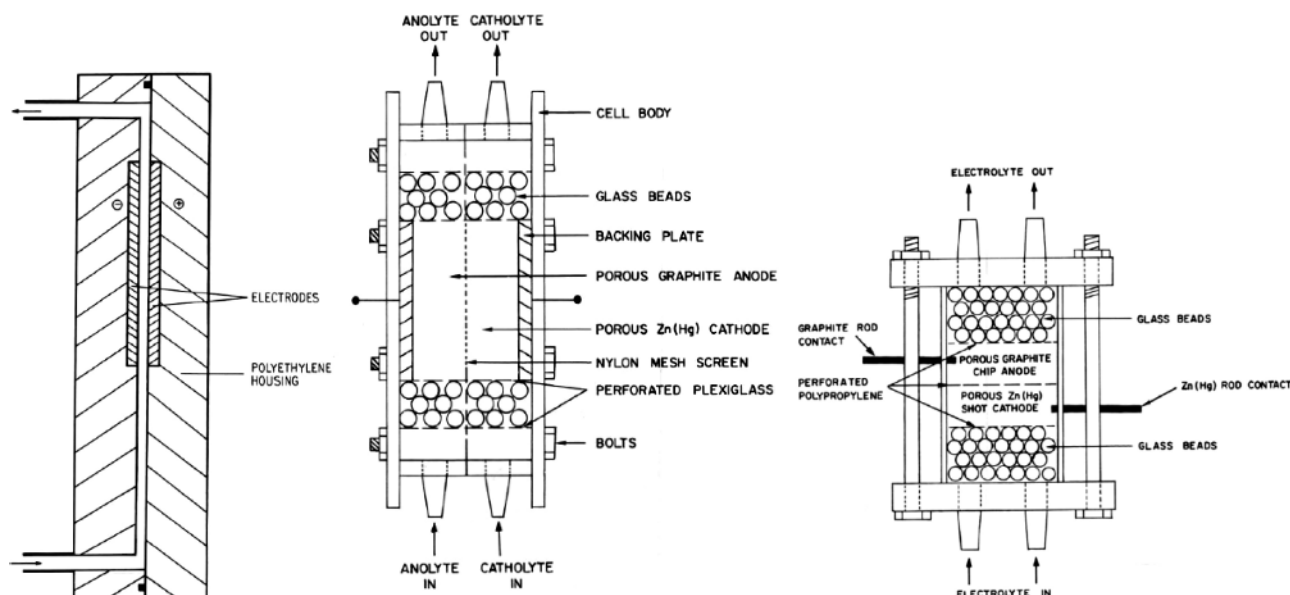
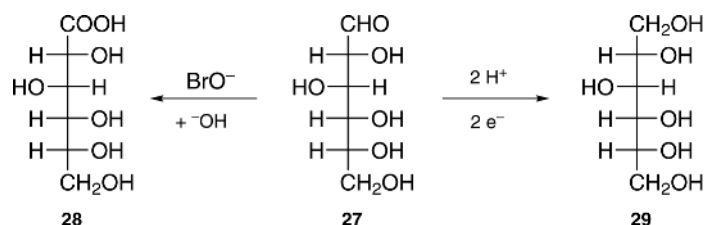


Figure 8. Three ECMR's developed for the paired synthesis of **28** and **29**. Left – Parallel plate configuration; Centre – Packed bed cell with perpendicular flow; Right – Packed bed cell with parallel flow. (With kind permission from Springer Science+Business Media: ref. [33])

Scheme 10. Paired synthesis of **28** and **29** from glucose **27**



3.3. Undivided Cell with a Segmented Anode. Rode et al. [30] conducted design calculations for a segmented thin gap cell. They concluded that if a high reagent conversion per single pass of the cell is required, much higher current density can be achieved in a segmented electrode ECMR.

Attour et al. [31] have reported the selective oxidation of 4-methylanisole **25** (Scheme 9) in an undivided cell fabricated on the basis of the theoretical calculations presented by Rode et al. [30] It was made of a stainless steel cathode, and a segmented anode, comprising of ten glassy carbon anodes ($1 \times 1 \text{ cm}^2$) separated by 1 mm wide insulated sections (Figure 7) and although the anode was segmented, all the carbon tiles were connected together for the experiments so the cell voltage remained uniform. The authors investigated an industrially important reaction and varied factors such as supporting electrolytes and their concentrations, flow rates, applied current, and were able to selectively oxidise **25** to **26** with an almost complete conversion of **25** and a selectivity of over 85% compared to 68% in an industrial cell. They were also able to substantially reduce the concentration of the supporting electrolyte (potassium fluoride) from 0.1 M in batch [32] to 0.01 M in flow.

3.4. Undivided Packed Bed Cells. Johnson et al. [33] have described and compared the paired synthesis of gluconic acid **28** and sorbitol **29** from glucose **27** (Scheme 10) in both, a parallel plate and packed bed cells. The parallel plate reactor (Figure 8, left) was formed from 2 plate electrodes (50 cm^2) and separated by a 3 mm gap, so by definition, not a microreactor. The electrode materials were graphite and amalgamated zinc or lead. To ensure that the flow was well developed before the reaction took place, a long entry channel was built into the device.

The packed bed device had a perpendicular arrangement for the current flow and solution flow (Figure 8, centre), and the

last (Figure 8, right) had a parallel flow arrangement. In the former, the packed beds ($9 \times 3 \times 1.5 \text{ cm}$) were insulated from each other by a nylon mesh. At the entrance and exit to the electrode compartment were placed glass beads (5 mm) to ensure uniform flow through the device and reference electrodes were inserted through the body into the cathodic compartment. In the parallel flow device, the packed bed electrodes were 5.7 cm in diameter and 1.2 cm thick and were separated by perforated polypropylene discs between a nylon mesh, and again the device had reference electrodes inserted through the body of the device. Both of the cells were packed with 0.5 cm zinc shots for the cathode, while the anode compartment was packed with cylindrical shaped graphite chips (0.3 cm diameter, 0.3 cm length).

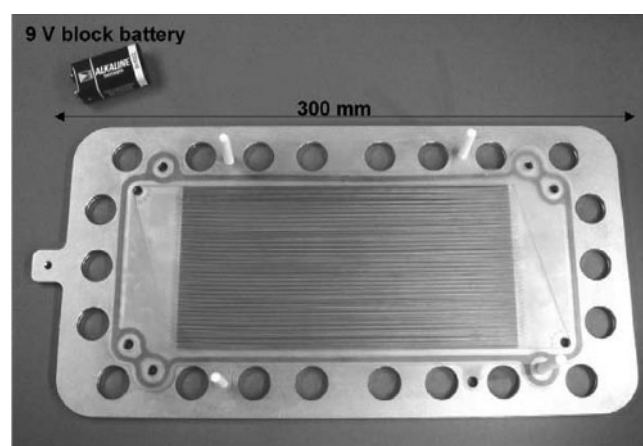
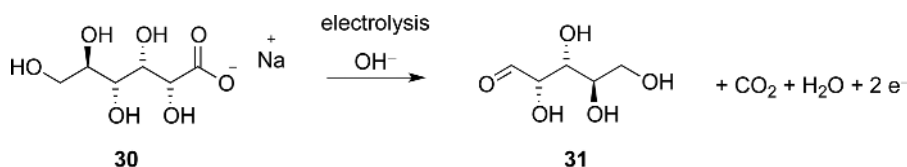


Figure 9. Photograph of the micro channel and frame of the ECMR (Reprinted from ref. [7] with permission from Elsevier)

Scheme 11. Reaction of sodium *D*-gluconate **30** to *D*-arabinose **31**

Optimum results achieved for the parallel plate reactor were 50% and 23% for **28** and **29**, respectively. As the substrate for both reactions was glucose **27**, the maximum yield for each product was 50%. The lower yield of **29** was “tentatively” ascribed to **29** building up in the circulating system as electrolyses were carried out in a batch recycling mode. This build up had an inhibitory effect on the reduction of glucose. Reactions carried out in both of the packed bed cells show that current efficiencies for the formation of **29** are the same as those from the parallel plate reactor, while the current efficiency for **28** is comparable to that of the parallel plate reactor for the packed bed with parallel flow, which is approximately 15% higher than that for the perpendicular flow device. The reasons for this were not known but the lower current efficiencies for the formation of **28** in the perpendicular flow device was attributed to the possibility of the transfer of electro-generated bromine from the anode to the cathode and being subsequently reduced.

3.5. Integrated Electrochemical Synthesis and Chromatographic Separation. An ECMR constructed by Ziogas et al. [34] was developed using the oxidation of 4-methylanisole **25** (Scheme 9). The reactor had two solid plate electrodes, a glassy carbon anode and a stainless steel cathode separated by a PEEK spacer. The spacer was constructed by wet chemical etching and laser cutting techniques. This allowed the authors to create 27 parallel channels within the device. They report that they were able to achieve selectivities of >90% and almost quantitative current efficiencies without supporting electrolyte, reducing

operating costs and after reaction work-up. The ratio of the electrode surface area to cell volume is reported to be about 400 times greater than that for bipolar electrodes, and about 20 times higher compared to chemical fixed-bed reactors.

This reactor was then altered for integration into a simulated moving bed (SMB) chromatographic technique subsequent to electrochemical synthesis reported by Küpper et al. [7] To increase the productivity of the electrochemical cell, the electrode area had to be increased to achieve higher flow rates while maintaining the optimum current density. This in turn led to elongation of the reactor channels. The reactor also had to be capable of achieving a flow rate of at least 10 ml min⁻¹ to be comparable to a typical SMB plant, and also to be able to operate at pressures up to 30 bar. The ECMR contains 75 parallel micro-channels with a channel length of 189 mm and electrodes 189 x 98 mm² (Figure 9). Once completed, the ECMR was capable of being used as a divided/undivided cell and operated in mono/bipolar modes. It was proven to be able to withstand pressures of up to 35 bar and flow rates of 10 ml min⁻¹ as described to be needed for integration with the SMB chromatography technique.

Once complete, case studies were carried out to prove the feasibility of the integrated process. The microreactor as mentioned can be run in divided and undivided modes and for the synthesis of *D*-arabinose **31** from sodium *D*-gluconate **30** (Scheme 11), the divided cell mode was chosen [35]. A schematic integrated system and a simulated concentration profile is shown in Figure 10. In the active area of the system, the concentration of the substrate decreases while the product concentration increases. Electrochemical reactions possess the unique ability to be switched on and off with the applied current, so once the reactors are switched off and changed to simulate moving bed chromatography, the reaction can be activated once more, making the combination of the two processes possible. The process is also modelled as a series process, with the ECMR's outside of the SMB process, which proved to be less efficient for product yield than the integrated one.

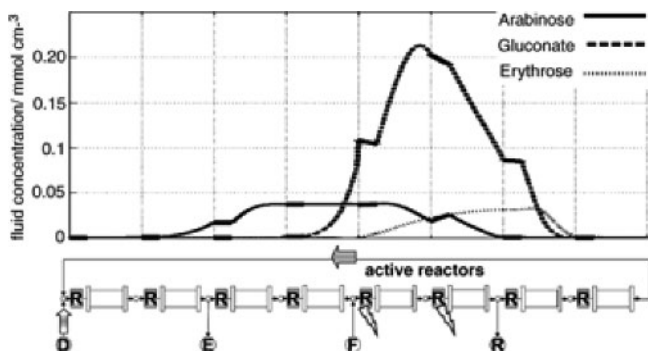


Figure 10. A schematic representation of an integrate ECMR-SMB synthesis and chromatographic separation process with a superimposed simulation of product concentration. The lightning bolts show the two active ECMR's, F: feedstock entry, E: extract collection, R: raffinate, D: desorbent. (With kind permission from Springer Science+Business Media: ref. [35])

4. Divided Cell Microreactor Synthesis

For divided cell electrolysis, advanced cell designs are necessary due to the nature of having to keep the two electrode compartments separate. In a divided cell for both batch and flow processes, the solutions contained in either the anodic or cathodic chambers are separated by a diaphragm or membrane. This can be either to keep both the solutions separate during electrolysis (so the reaction products are unable to react at the other electrode), or allow ions to diffuse through to the other chamber.

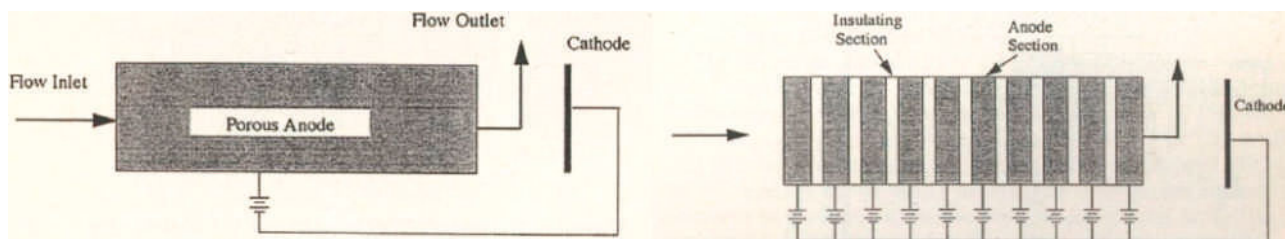
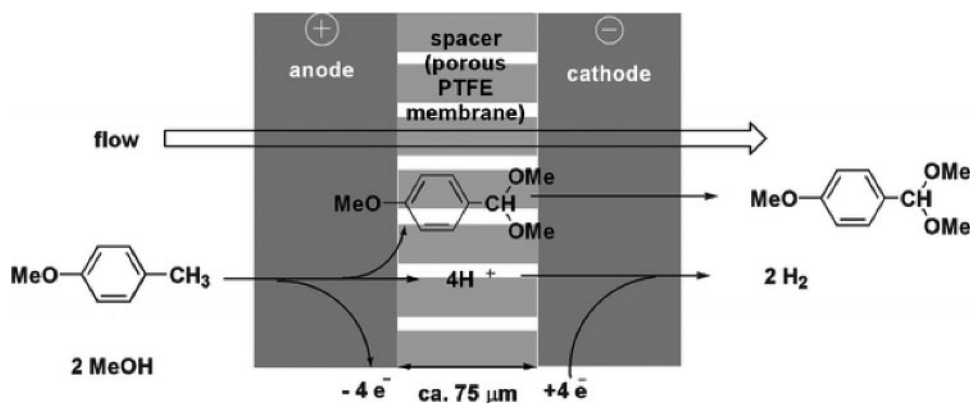


Figure 11. Single (left) and multisection porous electrode (right) configurations for electrochemical synthesis (Reproduced by permission of The Electrochemical Society [36])

Scheme 12. A schematic diagram for the anodic methoxylation of *p*-methoxytoluene in a divided ECMR (Reproduced from ref. [38] with permission of the Royal Society of Chemistry)

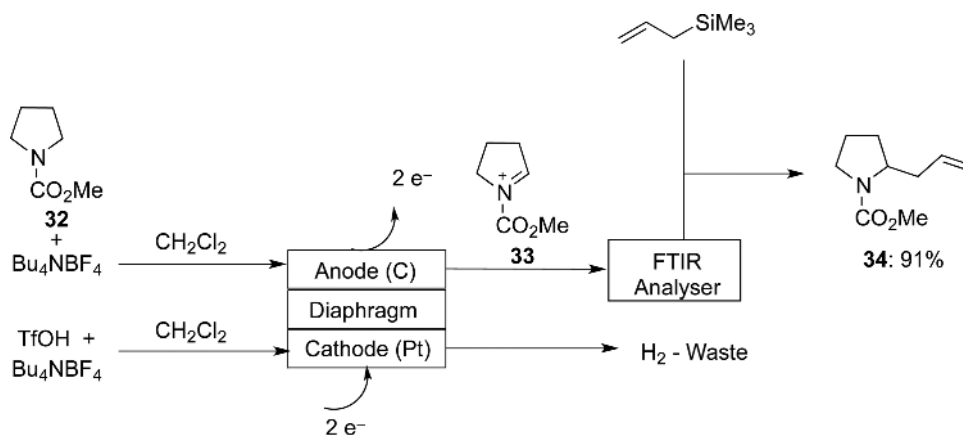


This type of cell is much more efficient at keeping the reaction selective due to the divided nature of the cell. [1,13,14]

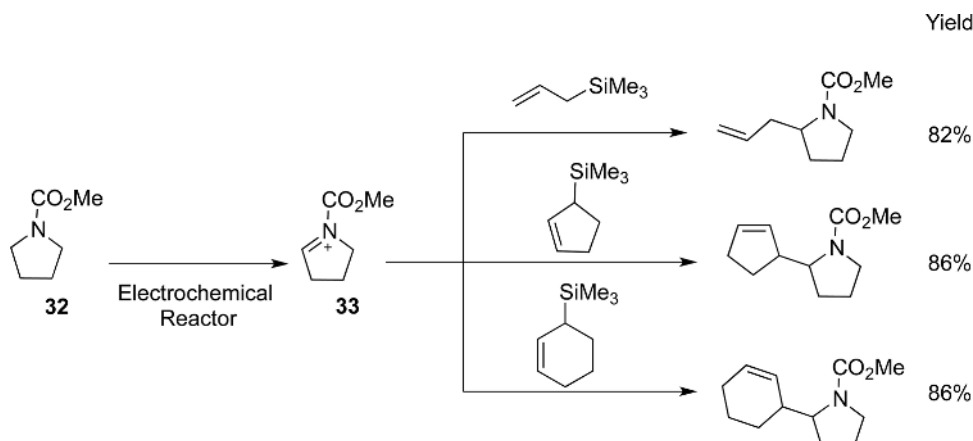
4.1. Porous Electrodes. Matlosz et al. [36,37] have reported a study comparing a single porous electrode system (Figure 11, left) with a multisection electrode consisting of ten porous graphite electrodes (Figure 11, right) for the synthesis of *D*-arabinose (Scheme 11). Their results indicate that the current efficiency for the reaction can be significantly improved by a factor of 2–2.5 when the number of electrodes is increased from one to ten. The improved performance can be attributed to greater uniformity of the current density distribution throughout the cell. However, a more complex design is needed for the cell as each electrode has its own current generator.

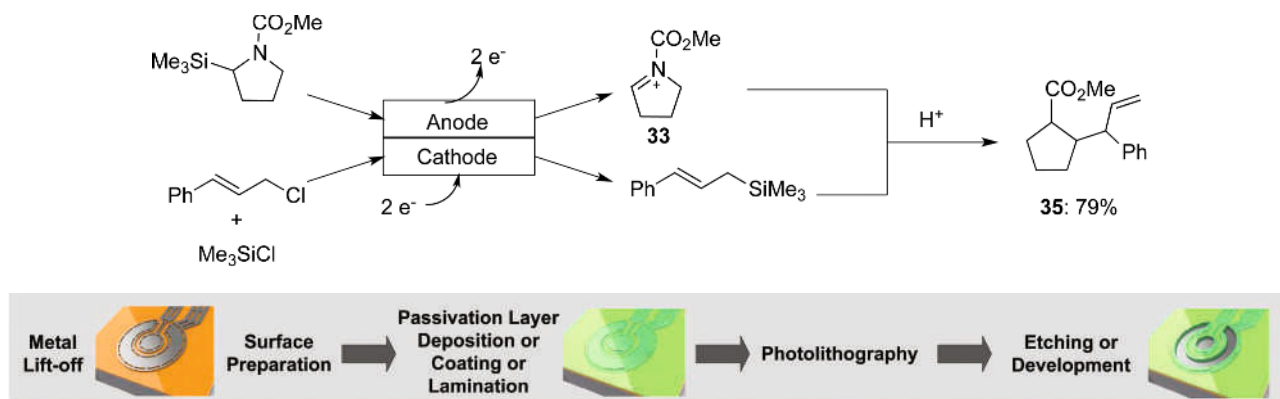
4.2. Perpendicular Current/Solution Flow. Yoshida et al. [38] developed an electrochemical microreactor for divided cell electrolysis. Their device was constructed from two carbon fibre electrodes separated by a porous membrane (Scheme 12). They chose to study the methoxylation of *p*-methoxytoluene as a test reaction because it is a well-known process and industrially important. The process is essentially the same as in a batch divided cell, the substrate enters the anodic chamber of the device and is oxidised, the acetal formed along with the generated protons move through the porous membrane into the cathodic chamber where the product leaves the device and hydrogen is generated from proton reduction. The authors were able to achieve yields of more than 90% with a current of 11 mA.

Scheme 13. Schematic representation of the “cation flow” method [40]



Scheme 14. Combinatorial chemistry with the “cation flow” method [41]



Scheme 15. Paired electrosynthesis using a divided ECMR and the “cation flow” method [41]**Figure 12.** General procedure for constructing interdigitated band electrodes (Reproduced from ref. [45] with permission of The Royal Society of Chemistry)

4.3. “Cation Flow” and Combinatorial Syntheses. Yoshida et al. [39] also developed an interesting procedure based on the “cation pool” method that they had previously developed in batch chemistry, the electrochemical formation of highly reactive carbocations and their subsequent reactions with nucleophiles. The “cation flow” method has been developed using the same principles [40]. Carbamates **32** were chosen as substrates because they had developed the “cation pool” method using these substrates. The substrate with a supporting electrolyte was fed into the anodic chamber of the device and trifluoromethanesulfonic acid as a proton source into the cathodic chamber. The *N*-acyliminium cation **33** is continuously generated and exits the device to be analysed online by infrared analysis to monitor the formation of **33** due to the higher wavenumber associated with the positive charge on the nitrogen atom adjacent to the carbonyl group, a subsequent combination with a nucleophile gives the desired product **34** (Scheme 13) [4]. This electrolysis proceeds without electrolyte using a perpendicular current/solution flow system.

This principle was then taken further, not only using different cation sources and nucleophiles, but also to achieve continuous sequential combinatorial chemistry [39]. This is achieved by a simple switching of the flow of **33** into separate streams of nucleophiles leading to different products formed in parallel as shown in Scheme 14 [4].

This methodology was used to complete different reactions and not just to vary substrates and nucleophiles. A selective Friedel-Crafts monoalkylation, when carried out using a micro-mixer instead of a batch reactor, yielded monoalkylated product in up to 92% with 4% of dialkylated product. Compared to a flask reaction, the yields were 37% and 32%, respectively [42]. Diels-Alder reactions [43], as well as controlled/living cationic polymerization reactions were also successfully undertaken [4,44].

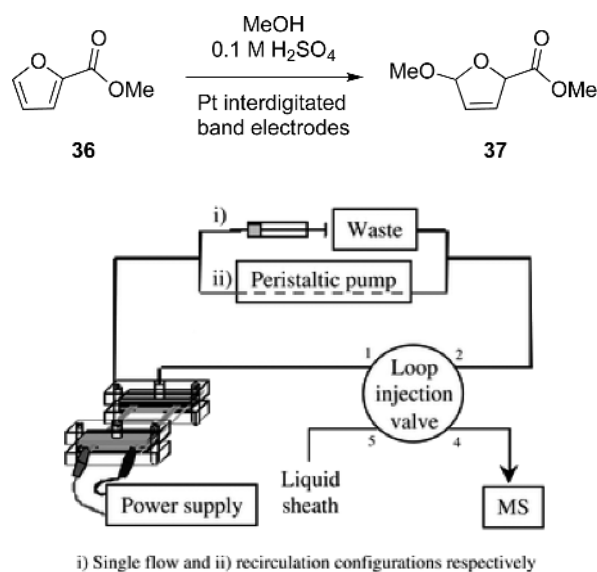
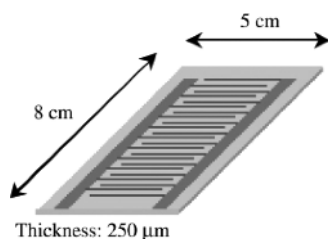
Another example from the Yoshida group involves paired electrosynthesis in a divided cell [41]. It is an interesting

example because the *N*-acyliminium ion **33**, generated by anodic oxidation in the anodic compartment, was reacted with the product formed from the cathodic chamber in a subsequent reaction, they were also able to directly react the cation with a substrate that has been simultaneously reduced in the cathodic chamber once leaving the device and combined. A good yield was achieved for the example shown (Scheme 15).

5. Interdigitated Band Electrodes

Interdigitated band electrodes are possibly less used in organic synthesis, they are, however, quite popular for electrochemical sensing applications [45]. Complex electrode shapes can be developed via photolithography as shown in Figure 12. Methods such as screen printing using a metallic ink can be just as successful.

Belmont et al. [46] applied microelectrode technology to produce large scale electrodes with micrometer inter-electrode distances. This was achieved at a low cost by screen printing the electrode designs using a platinum paste on alumina (Figure 13). The porosity of the electrodes was characterised by electrochemical means and implied that the active surface area of the electrodes is 54 times bigger than their geometric size. When the inter-electrode distance

Scheme 16. The anodic methoxylation of 2-methylfuroate **36****Figure 14.** A schematic representation of the ceramic microreactor with online mass spectrometry (Reproduced from ref. [47] with permission of The Royal Society of Chemistry)**Figure 13.** An example of an interdigitated band electrode array (Reproduced from ref. [47] with permission of The Royal Society of Chemistry)

was reduced, the yield, current efficiency and overall energy consumption improved using the methoxylation of furan as a test reaction.

Girault et al. [47] reported a ceramic microreactor that was used to investigate the methoxylation of 2-methylfuroate **36** (Scheme 16). The band electrodes were fabricated using a screen printing method. The reactor was sealed using a sintering technique at 850 °C and an online monitoring system by incorporating a mass spectrometer into the system was connected directly to the outlet of the microreactor to analyse the product **37** generated (Figure 14).

6. Conclusions

There are also many other reactions involving paired and coupled electrode processes that have been carried out in ECMR's, which are covered in a comprehensive review by Marken et al. [9]

Combining electrochemistry and microreactors has been successful in many cases and is a viable alternative to conventional electrochemistry where difficulties such as poor heat/mass transfer properties are encountered. In addition, electroorganic flow chemistry can deliver high throughputs of valuable compounds, ideal to pharmaceutical and other industries. Scaling up is also easily achievable once the initial process has been optimised in an ECMR. The use of one or more ECMR's in parallel allows efficient continuous processing. The absence of supporting electrolytes in ECMR's is an interesting prospect as it simplifies the reaction work-up, allowing the creation of a "greener" reaction while keeping the overall costs of the process down. The technology, now no longer in its infancy will have dramatic effects on conventional methods and plays an important part in what is now becoming a major goal in all areas of chemistry.

References

1. Speiser, B. *Encyclopedia of Electrochemistry Volume 8*, Wiley-VCH, 2004.
2. Sequeira, C. A. C.; Santos D. M. F. *J. Brazil. Chem. Soc.* **2009**, *20*, 387.
3. a) Utley, J. *Chem. Soc. Rev.* **1997**, *26*, 157; b) Yoshida, J.-i.; Kataoka, K.; Horcajada, R.; Nagaki, A. *Chem. Rev.* **2008**, *108*, 2265.
4. Yoshida, J.-i. *The Electrochemical Society Interface*, **2009**, Summer, 40.
5. a) Elizarov, A. M.; van Dam, R. M.; Shin, Y. S.; Kolb, H. C.; Padgett, C.; Stout, D.; Shu, J.; Huang, J.; Daridon, A.; Heath, J. R. *J. Nucl. Med.* **2010**, *51*, 282; b) Lee, C.-C.; Sui, G.; Elizarov, A.; Shu, C. J.; Shin, Y.-S.; Dooley, A. N.; Huang, J.; Daridon, A.; Wyatt, P.; Stout, D.; Kolb, H. C.; Witte, O. N.; Satyamurthy, N.; Heath, J. R.; Phelps, M. E.; Quake, S. R.; Tseng, H. R. *Science* **2005**, *310*, 1793; c) Watts, P.; Pascali, G.; Salvadori, P. A. *J. Flow Chem.* **2012**, *2*, 37.
6. Roberge, D. M.; Ducry, L.; Bieler, N.; Cretton, P.; Zimmermann, B. *Chem. Engin. Tech.* **2005**, *28*, 318.
7. Küpper, M.; Hessel, V.; Löwe, H.; Stark, W.; Kinkel, J.; Michel, M.; Schmidt-Traub, H. *Electrochim. Acta*, **2003**, *48*, 2889.
8. Autze, V.; Hohmann, M.; Stimer, W.; Schwalbe, T. *Org. Proc. Res. Dev.* **2004**, *8*, 440.
9. Paddon, C. A.; Atobe, M.; Fuchigami, T.; He, P.; Watts, P.; Haswell, S. J.; Pritchard, G. J.; Bull, S. D.; Marken, F. *J. Appl. Electrochem.* **2006**, *36*, 617.
10. Ziogas, A.; Kolb, G.; O'Connell, M.; Attour, A.; Lapique, F.; Matlosz, M.; Rode, S. *J. Appl. Electrochem.* **2009**, *39*, 2297.
11. Stradiotto, N. R.; Yamanaka, H.; Zanoni, M. V. B. *J. Braz. Chem. Soc.* **2003**, *14*, 159.
12. Janata, J.; Bezegh, A. *Anal. Chem.* **1988**, *60*, R62.
13. Lund H.; Hammerich, O. *Organic Electrochemistry*, 4th edn.; CRC Press, 2001.
14. Shono, T. *Electroorganic Synthesis*, Academic Press Limited, 1991.
15. Cheng, P. C.; Nonaka, T. *J. Electroanal. Chem.* **1989**, *269*, 223.
16. a) Nonaka, T.; Cheng, P.; Uneyama, K. *Denki Kagaku* **1991**, *59*, 427; b) K. Arai, K. Watts, T. Wirth, *ChemistryOpen* **2014**, *3*, in press. DOI: 10.1002/open.201300039
17. Löwe, H.; Ehrfeld, W. *Electrochim. Acta* **1999**, *44*, 3679.
18. Paddon, C. A.; Pritchard, G. J.; Thiemann, T.; Marken, F. *Electrochem. Commun.* **2002**, *4*, 825.
19. Horii, D.; Atobe, M.; Fuchigami, T.; Marken, F. *Electrochem. Commun.* **2005**, *7*, 35.
20. He, P.; Watts, P.; Marken, F.; Haswell, S. J. *Electrochem. Commun.* **2005**, *7*, 918.
21. He, P.; Watts, P.; Marken, F.; Haswell, S. J. *Angew. Chem. Int. Ed.* **2006**, *45*, 4146.
22. He, P.; Watts, P.; Marken, F.; Haswell, S. J. *Lab Chip* **2007**, *7*, 141.
23. He, P.; Watts, P.; Marken, F.; Haswell, S. J. *Green Chem.* **2007**, *9*, 20.
24. Watts, K.; Gattrell, W.; Wirth, T. *Beilstein J. Org. Chem.* **2011**, *7*, 1108.
25. Kuleshova, J.; Hill-Cousins, J. T.; Birkin, P. R.; Brown, R. C. D.; Pletcher, D.; Underwood, T. J. *Electrochim. Acta* **2011**, *56*, 4322.
26. Kuleshova, J.; Hill-Cousins, J. T.; Birkin, P. R.; Brown, R. C. D.; Pletcher, D.; Underwood, T. J. *Electrochim. Acta* **2012**, *69*, 197.
27. Roth, G. P.; Stalder, R.; Long, T. R.; Sauer, D. R.; Djuric, S. W. *J. Flow Chem.* **2013**, *3*, 34.
28. Kashiwagi, T.; Elsler, B.; Waldvogel, S. R.; Fuchigami, T.; Atobe, M. *J. Electrochem. Soc.* **2013**, *160*, G3058.
29. Kashiwagi, T.; Amemiya, F.; Fuchigami, T.; Atobe, M. *Chem. Commun.* **2012**, *48*, 2806.
30. Rode, S.; Altmeyer, S.; Matlosz, M. *J. Appl. Electrochem.* **2004**, *34*, 671.
31. Attour, A.; Rode, S.; Ziogas, A.; Matlosz, M.; Lapique, F. *J. Appl. Electrochem.* **2008**, *38*, 339.
32. Attour, A.; Rode, S.; Bystron, T.; Matlosz, M.; Lapique, F. *J. Appl. Electrochem.* **2007**, *37*, 861.
33. Pintauro, P. N.; Johnson, D. K.; Park, K.; Baizer, M. M.; Nobe, K. *J. Appl. Electrochem.* **1984**, *14*, 209.
34. Ziogas, A.; Löwe, H.; Küpper, M.; Ehrfeld, W. *Microreaction Technology: Industrial Prospects*, Proceedings of the Third International Conference on Microreaction Technology (IMRET 3), Springer-Verlag, 2000; pp. 136.
35. Michel, M.; Schmidt-Traub, H.; Ditz, R.; Schulte, M.; Kinkel, J.; Stark, W.; Küpper, M.; Vorbrod, M. *J. Appl. Electrochem.* **2003**, *33*, 939.
36. Vallières, C.; Matlosz, M. *J. Electrochem. Soc.* **1999**, *146*, 2933.
37. Matlosz, M. *J. Electrochem. Soc.* **1995**, *142*, 1915.
38. Horcajada, R.; Okajima, M.; Suga, S.; Yoshida, J.-i. *Chem. Commun.* **2005**, 1303.
39. Yoshida, J.-i.; Suga, S. *Chem. Eur. J.* **2002**, *8*, 2650.
40. Suga, S.; Okajima, M.; Fujiwara, K.; Yoshida, J.-i. *J. Am. Chem. Soc.* **2001**, *123*, 7941.
41. Suga, S.; Okajima, M.; Fujiwara, K.; Yoshida, J.-i. *QSAR Comb. Sci.* **2005**, *24*, 728.
42. Suga, S.; Nagaki, A.; Yoshida, J.-i. *Chem. Commun.* **2003**, 354.
43. Suga, S.; Nagaki, A.; Tsutsui, Y.; Yoshida, J.-i. *Org. Lett.* **2003**, *5*, 945.
44. Nagaki, A.; Kawamura, K.; Suga, S.; Ando, T.; Sawamoto, M.; Yoshida, J.-i. *J. Am. Chem. Soc.* **2004**, *126*, 14702.
45. Temiz, Y.; Ferretti, A.; Leblebici, Y.; Guiducci, C. *Lab Chip* **2012**, *12*, 4920.
46. Belmont, C.; Girault, H. H. *J. Appl. Electrochem.* **1994**, *24*, 719.
47. Mengeaud, V.; Bagel, O.; Ferrigno, R.; Girault, H. H.; Haider, A. *Lab Chip* **2002**, *2*, 39.